

# Challenges in Optimization of a Stationary Tomographic Molecular Breast Imaging System

Kjell Erlandsson, Andras Wirth, Kris Thielemans, *Senior Member, IEEE*, Ian Baistow, Alexander Cherlin, *Member, IEEE*, Brian F. Hutton, *Senior Member, IEEE*

**Abstract**— A prototype Molecular Breast Imaging (MBI) system is currently under development, motivated by the need of a practical low-dose system for use in patients with dense breast tissue, where conventional mammography is limited. The system is based on dual opposing CZT detector arrays and multi-pinhole collimators which allow for multiplexing in the projection data. We have performed optimization of various design parameters based on either contrast-to-noise ratio (CNR) in the reconstructed images or area under the localization receiver operating characteristics curve (LROC-AUC) obtained using the scan statistic model. The optimizations were based on simulated data, and the parameters investigated were pinhole size and opening angle, pinhole separation and collimator-to-detector separation. The two optimization approaches resulted in similar design parameters, allowing for reconstruction of tomographic images with high CNR and lesion detectability, which can lead to a reduced dose or scan time as compared to planar MBI.

## I. INTRODUCTION

MOLECULAR Breast Imaging (MBI) using dual opposing detectors has been shown to have high sensitivity for cancer detection, even in patients with dense breasts where x-ray mammography can be limited [1]. However, relatively high radiation dose is currently hindering its adoption as a screening modality. We are developing a stationary low-dose MBI system based on dual opposing cadmium zinc telluride (CZT) detectors with high intrinsic resolution and capability for depth-of-interaction (DOI) estimation [2]-[3]. The system utilizes densely packed multi-pinhole (MPH) collimators which result in significant multiplexing (overlap of projections from different pinholes, MX). The 3D reconstruction relies on use of de-multiplexing algorithms, aided by the DOI information [4]. Previous MPH systems either avoid MX and use detector scanning motion to improve sampling [5], or utilize a shutter mechanism in order to obtain both MX and non-MX data [6]. Our proposed system is stationary, avoiding complex mechanics and is suitable for breast screening. The objective of this paper is to describe the simulation studies that were performed to optimize the design of the system.

## II. METHODS

We performed computer simulations for a system consisting of two 7.3 mm thick and 16 cm x 16 cm wide CZT detectors with a pixel size and DOI resolution of 1 mm. The collimators

were made of 5 mm thick Tungsten with arrays of square-shaped pinholes. The parameters investigated were pinhole size, opening angle and separation. Collimator-to-detector separation was fixed to a value obtained at an earlier stage. Most of the investigated design configurations resulted in some degree of MX. MX leads to higher sensitivity and improved sampling, but also to uncertainty regarding the path of each detected photon and possible artefacts, and has for this reason often been avoided in the past. We incorporated a de-MX procedure into the OSEM based tomographic reconstruction algorithm [4]. Two different approaches were implemented for the purpose of optimizing the collimator design.

### A. Contrast to Noise Ratio

The first approach was based on maximization of the contrast-to-noise ratio (CNR). A hot-lesion phantom was designed based on a previously proposed 2D phantom [7]. The phantom was 6 cm thick and contained 18 spherical lesions with 3 to 8 mm diameter and target-to-background contrast of 10 to 130, placed at a depth of 15 mm. Projection data were generated by analytical forward projection and Poisson noise was added corresponding to the number of counts acquired over 5 min. Images were reconstructed with 1 to 5 iterations and 3 sub-sets. Noise estimates were obtained as the coefficient of variation (COV) in a uniform region of the phantom, and CNR was calculated for each lesion. The average CNR over all 18 lesions was used as the outcome metric to be maximized. An extra complication is that CNR depends on the number of iterations used in the reconstruction. Looking at contrast vs. noise curves for a range of parameter values, the curves did not always overlap in terms of their range of contrast and noise values, making direct comparison difficult (see Figure 1). We therefore compared curves for two adjacent parameter values at a time in order to find the best choice.

### B. Numerical Observer

The second approach used was based on a numerical observer study using the scan statistics model [8]. For this purpose, we simulated data for a phantom containing 20 spherical lesions, all with a diameter of 5 mm and a tumor-to-background ratio (TBR) of 10. The lesions were placed at random locations in the phantom. Data were generated and reconstructed as described above. We then generated

Manuscript received November 19, 2021. The Institute of Nuclear Medicine is supported by the NIHR University College London Hospitals Biomedical Research Centre. Kromek are supported by an Innovate UK grant (104296).

K. Erlandsson, K. Thielemans and B. F. Hutton are with The Institute of Nuclear Medicine (INM), University College London, London, UK. (e-mail: k.erlandsson@ucl.ac.uk)

A. Wirth, I. Baistow and A. Cherlin are with Kromek Ltd, County Durham, UK.

localization receiver operating characteristics (LROC) curves and calculated the area under the curve (AUC), which was the outcome measure to be maximized. Optimization was performed in terms of the parameters mentioned above as well as the number of iterations.

### III. RESULTS

Figure 2 shows an example of data from the CNR-based optimisation. After rescaling of the CNR values in (a), we found that the best choice was a pinhole aperture of 1.5 or 2 mm, which is different from what would be obtained by just looking at the highest CNR value. In (b) rescaling was no necessary, and the best choice was a pinhole separation of 9 mm. The optimal configuration, based on a large number of simulations, was defined by the following parameters: pinhole aperture = 1.75 mm, pinhole separation = 9 mm, pinhole opening angle (including penumbra) = 85°. This configuration resulted in 64% multiplexed data.

Figure 3 shows data from the AUC-based optimisation, displaying the best results from a number of optimisation sequences, where one parameter at a time was change over a range of values. The overall best result was obtained for the following parameters: pinhole aperture = 2 mm, pinhole separation = 9 mm, pinhole opening angle = 80°. These values are close to those of the CNR-based optimisation.

Figure 4 shows one slice from the reconstructed phantom used in the CNR-optimization with both sub-optimal and optimal parameter. The former corresponds to a configuration with very little MX. It can be seen that the optimized parameters result in higher contrast.

### IV. DISCUSSION & CONCLUSIONS

When designing a detector system for MBI, the goal is to obtain images with high contrast and low noise-level in order to maximize the probability of detecting a lesion. One way to achieve this is to calculate the ratio of the two quantities (CNR) and find out when it is maximized. On the other hand, the use of numerical observers is a way of directly estimate the systems capability in terms of lesion detection. The downside with the AUC-based optimization was the necessity to choose a particular lesion size and TBR. In the CNR-based approach, a range of lesion sizes and contrasts were included. We found that it was important to take into account the number of iterations in order to avoid drawing the wrong conclusions.

In conclusion, we have optimized the geometry of a MBI system using two different approaches. The fact that two different optimization criteria gave similar results increased the credibility of the outcome.

### REFERENCES

- [1] Hruska CB, "Molecular Breast Imaging for Screening in Dense Breasts: State of the Art and Future Directions", *AJR*, **208**:275-83, 2017.
- [2] Cherlin A, Wirth A, Erlandsson K, Baistow I, Thielemans K, Hutton BF, "A new concept for a low-dose stationary tomographic Molecular Breast Imaging camera using 3D position sensitive CZT detectors",
- [3] Hutton BF, Erlandsson K, Wirth A, Baistow I, Thielemans K, Cherlin A, "Design of an ultra-low-dose, stationary, tomographic Molecular Breast

Imaging system", *Conference record, 2021 IEEE Nucl. Sci. Symp. & Med. Imag. Conf.*, 2021.

- [4] Erlandsson K, Wirth A, Baistow I, Thielemans K, Cherlin A, Hutton BF, "Novel approaches to reconstruction of highly multiplexed data for use in stationary low-dose molecular breast tomosynthesis", *Proceedings of the 16<sup>th</sup> International Meeting on Fully 3D Image Reconstruction in Radiology and Nuclear Medicine*, Leuven, Belgium, 2021.
- [5] van Roosmalen J, Goorden MC, Beekman FJ, Molecular breast tomosynthesis with scanning focus multi-pinhole cameras, *Phys. Med. Biol.*, 61: 5508-28, 2016.
- [6] Zeraatkar N, Auer B, Kalluri KS, May M, Momsen NC, Richards RG, Furenlid LR, Kuo PH, King MA, "Improvement in sampling and modulation of multiplexing with temporal shuttering of adaptable apertures in a brain-dedicated multi-pinhole SPECT system", *Phys. Med. Biol.*, 66: 065004, 2021.
- [7] Long Z, Conners AL, Hunt KN, Hruska CB, O'Connor MK, "Performance characteristics of dedicated molecular breast imaging systems at low doses", *Med. Phys.*, **43**(6): 3062-70, 2016.
- [8] Popescu LM, Lewitt RM, "Small nodule detectability evaluation using a generalized scan-statistic model", *Phys. Med. Biol.*, **51**:6225-44, 2006.

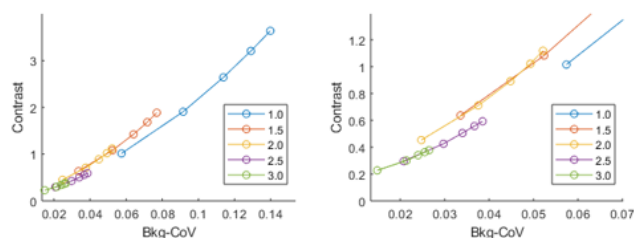


Fig. 1. Contrast vs. noise curves for different pinhole apertures (1 to 3 mm, 1 to 5 iterations). The graph on the left is a blow-up of part of one on the right. As all curves do not overlap, direct comparison is difficult.

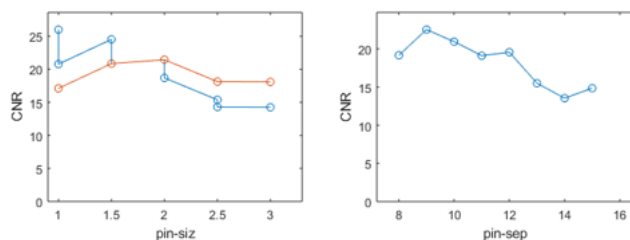


Fig. 2. CNR vs. pinhole aperture (a) and pinhole separation (b). The red curve in (a) represents rescaled values for comparison of non-overlapping contrast-noise curves (see Fig. 1).

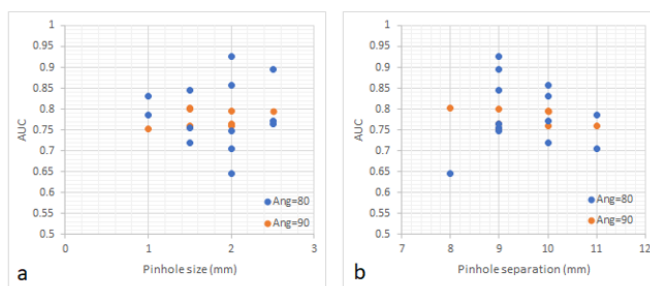


Fig. 3. Result from the AUC-based optimization, showing the best configurations for a number of optimization sequences with pinhole opening angles of 80° (blue dots) and 90° (red dots).

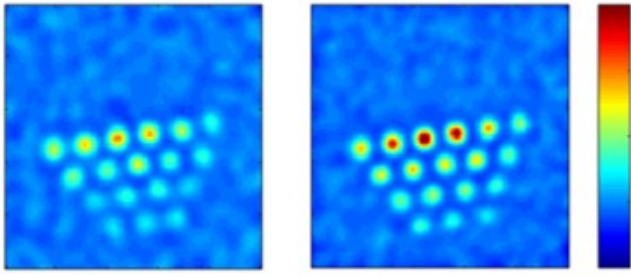


Fig. 4. Reconstructed images of phantom used in the CNR-optimisation, with sub-optimal (left) and optimised parameters (right).